AIAA 81-4215

Harmonic Optimization of a Periodic Flow Wind Tunnel

John P. Retelle Jr.*
United States Air Force Academy, Colo.
James M. McMichael†
National Bureau of Standards, Gaithersburg, Md.
and
Donald A. Kennedy‡
University of Colorado, Boulder, Colo.

This work describes a wind-tunnel modification designed to superpose on the mean velocity sinusoidal longitudinal velocity fluctuations with minimal harmonic content. The technique is presented in light of a theoretical analysis of the low-frequency performance illustrating how harmonic suppression can be achieved with this particular design. Velocity fluctuations are produced by a system of primary rotating vanes and a bypass containing a secondary set of rotating vanes. Experimental data on tunnel performance are also presented. A significant reduction of the second harmonic content of the freestream velocity oscillations was achieved by adjustment of the bypass flow.

Nomenclature

A,B,C,D = parameters defined by Eqs. (15) and (17)
$A(x)$ = local cross-sectional area of duct
a_n = Fourier coefficient of nth harmonic of fluctuating pressure coefficient for rotating vanes
b_n = Fourier coefficient of nth harmonic of fluctuating velocity
C_{ab} = pressure drop coefficient as defined by Eq. (2)
c = airfoil chord length
F_1,F_2 = pressure drop coefficients for rotating vanes
f_1,f_2 = normalized fluctuation of pressure drop coefficient for rotating vanes
G,H = parameters defined by Eq. (20)
K_{ab} = effective pressure drop coefficient defined by Eq. (4)
K_1,K_2 = pressure drop coefficients
$\hat{K}$ = kurtosis of u_1'
k = reduced frequency $c\omega/2\bar{U}_1$
$L/2$ = width of opening in adjustable vent for bypass system
N = velocity amplitude ratio, $\Delta U_1/\bar{U}_1$
n = Fourier index
p = pressure
Δp_f = fan pressure rise
p_f = fluctuation in fan pressure rise
Q = total volume flowrate through fan
Q_1 = test action volume flowrate
Q_2 = bypass volume flowrate
q_1,q_2 = normalized flowrate (or velocity) fluctuation
R,S = parameters defined by Eqs. (15) and (19)
Re = Reynolds number $\rho\bar{U}_1c/\mu$
$\hat{S}$ = skewness of u_1'
T = period of oscillation
t = time
$\bar{U}_1$ = mean velocity in test section
ΔU_1 = peak velocity amplitude
u_1' = longitudinal test-section velocity fluctuation
V_1,V_2 = voltages corresponding to first and second harmonic in velocity fluctuation
x = distance along duct axis
α_{ab} = parameter defined by Eq. (4)
β = negative of slope of fan curve
γ = local effective wall skin friction coefficient per unit area
μ = dynamic viscosity
ω = circular frequency
ρ = air density
τ_1,τ_2 = time constants defined by Eq. (16)

Superscript

$(\bar{\ })$ = time average

Received Nov. 13, 1979; revision received March 5, 1981. This paper is declared a work of the U. S. Government and therefore is in the public domain.

*Major, USAF, Associate Professor, Department of Aeronautics.
†Mechanical Engineer, Fluid Engineering Division.
‡Associate Professor, Department of Aerospace Engineering Sciences.

I. Introduction

EXPERIMENTAL investigations of unsteady boundary-layer separation and dynamic stall have used unsteady variations of airfoil angle of attack,[1,2] freestream velocity,[3-5] or both.[6] Experiments using only velocity fluctuations simplify data acquisition because the airfoil is stationary while still producing unsteady phenomena resembling those on an airfoil oscillating in pitch. Unsteady effects, such as regions of unseparated reversed flow in the boundary layer, are known to depend upon the harmonic content of the velocity fluctuations in the freestream.[5] Hence, it is important to produce fluctuations as free as possible from unwanted harmonics.

The wind-tunnel modification analyzed and described in this paper was specifically designed to superpose on the mean velocity sinusoidal velocity fluctuations with minimal harmonic content. The technique is a variant of the rotating vane technique previously used by a number of investigators.[4,7-9] The primary disadvantage of the usual design using rotating vanes to periodically block the flow is that the effective (time dependent) pressure drop coefficient across these vanes contains a sharp cusp when the vanes rotate through the position of maximum blockage. Such a cusped waveform is characterized by substantial harmonic content. The novel feature of the present technique is that a secondary (bypass) set of rotating vanes provides periodic venting between the primary shutters and the fan. In effect, as shown in the next section, the coupled action of both sets of vanes provides a forcing function for the flow in the test section which contains no second harmonic when the bypass system is properly adjusted. Thus, at least at sufficiently low frequencies, velocity fluctuations can be produced which, in principle, are also free of second harmonics.

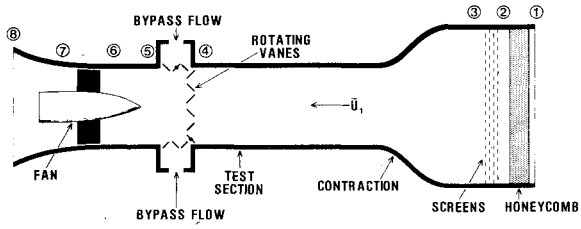

Fig. 1 Schematic of wind tunnel.

An additional benefit from the present technique is that the fan is allowed to operate with far less surging along its operating characteristic, thus preventing additional harmonic generation that would otherwise arise due to periodic stalling of the fan blades.

II. Wind-Tunnel Analysis

The wind-tunnel configuration shown schematically in Fig. 1 is described in detail in Sec. III. For the purpose of analysis it is sufficient to consider the wind tunnel to be composed of a primary flow path consisting of an entrance and settling chamber as shown, followed by the test section, primary vanes, fan, and diffuser, and a secondary flow path where outside air is admitted to the fan inlet through the secondary (bypass) vanes as also shown. Various stations along the primary path are indicated by number for reference.

The analysis to follow is essentially a lumped circuit analysis in which the station-to-station pressure drops are proportional to the square of the volumetric flow rate at any instant of time. For discrete elements such as screens, honeycombs, and vanes, this follows from the assumption of quasisteady, one-dimensional, incompressible flow, and Reynolds number independence. Thus, if $Q(t)$ is the volumetric flow rate given by

$$Q(t)=A(x)u(x,t) \tag{1}$$

where $A(x)$ is the cross-sectional area at position x along the duct, and $u(x,t)$ the local time (t) dependent velocity, then one may write for each discrete element,

$$p_a-p_b=C_{ab}Q^2(t) \tag{2}$$

where C_{ab} is an effective pressure-drop coefficient (proportional to the pressure-drop coefficient defined in terms of dynamic pressure), p the pressure, and a and b refer to appropriate arbitrary station numbers.

For distributed segments of the duct, lumped parameters can also be defined. Consider the one-dimensional, incompressible momentum equation

$$\frac{\partial u}{\partial t}+u\frac{u}{\partial x}=-\frac{\partial}{\partial x}\left(\frac{p}{\rho}\right)-\gamma(x)u^2 \tag{3}$$

where ρ is the air density and $\gamma(x)$ the local wall shear stress coefficient per unit area. Substituting Eq. (1) into Eq. (3) to eliminate $u(x,t)$, and integrating the result from station a to station b, one obtains

$$p_a-p_b=\alpha_{ab}\frac{dQ}{dt}+K_{ab}Q^2 \tag{4}$$

where

$$\alpha_{ab}=\rho\int_a^b\frac{dx}{A(x)}$$

and

$$K_{ab}=\rho/2\left[\frac{1}{A^2(x)}\right]_a^b+\rho\int_a^b\frac{\gamma(x)}{A^2(x)}dx$$

Let Q_1 denote the volume rate of flow in the test section, Q_2 the bypass flowrate, and Q the total volume flow through the fan. Thus,

$$Q_1+Q_2=Q \tag{5}$$

Let Δp_f denote the pressure rise across the fan. Since $p_1=p_8$, summing the pressure drops through the primary flow path, using Eqs. (2) and (4), yields

$$\Delta p_f=[K_1+F_1(t)]Q_1^2+\alpha_{15}\frac{dQ_1}{dt}+K_{58}Q^2+\alpha_{58}\frac{dQ}{dt} \tag{6}$$

where $K_1=K_{15}+C_{12}+C_{23}$, and $F_1(t)$ is the effective pressure drop coefficient for the primary rotating vanes.

Similarly, summing pressure drops through the secondary flow path yields

$$\Delta p_f=[K_2+F_2(t)]Q_2^2+K_{58}Q^2+\alpha_{58}\frac{dQ}{dt} \tag{7}$$

where $F_2(t)$ is the coefficient for the bypass vanes, and K_2 an adjustable pressure drop coefficient for the bypass inlet (described more fully in Sec. III). Equations (5-7) constitute a system of three equations in the three unknowns Q_1, Q_2, and Q.

Taking the sum and difference of Eqs. (6) and (7), using Eq. (5) to eliminate Q, one obtains

$$\Delta p_f=K_{58}(Q_1+Q_2)^2+\alpha_{58}\frac{d}{dt}(Q_1+Q_2)+(K_1+F_1)Q_1^2+\alpha_{15}\frac{dQ_1}{dt} \tag{8}$$

and

$$(K_1+F_1)Q_1^2+\alpha_{15}\frac{dQ_1}{dt}=(K_2+F_2)Q_2^2 \tag{9}$$

This system of nonlinear equations governs the dynamics of the wind tunnel in response to the forcing provided by the rotating vanes, i.e., by $F_1(t)$ and $F_2(t)$. To extract the salient performance features from these equations, they will now be linearized about a reference state established by the mean flow. Introducing mean and fluctuating quantities

$$\Delta p_f=\bar{\Delta}p_f+p_f(t)$$

$$F_1=\bar{F}_1[1+f_1(t)],\qquad F_2=\bar{F}_2[1+f_2(t)]$$

$$Q_1=\bar{Q}_1[1+q_1(t)],\qquad Q_2=\bar{Q}_2[1+q_2(t)]$$

where an overbar denotes a time-averaged variable, and fluctuation levels are restricted such that

$$|f_1|\sim|f_2|\sim|q_1|\sim|q_2|\ll 1$$

it is found that the mean flow is governed by the approximate equations

$$\bar{\Delta}p_f=K_{58}(\bar{Q}_1+\bar{Q}_2)^2+(K_1+\bar{F}_1)\bar{Q}_1^2 \tag{10}$$

$$(K_1+\bar{F}_1)\bar{Q}_1^2=(K_2+\bar{F}_2)\bar{Q}_2^2 \tag{11}$$

Neglecting second- and higher-order terms in fluctuating quantities, and representing the fan pressure fluctuation as

$$p_f(t) = -\beta(\bar{Q}_1 q_1 + \bar{Q}_2 q_2) \tag{12}$$

where $\beta > 0$ is minus the slope of the fan pressure-volume flow curve, the dynamic equations may be written as

$$[1+B+A(1+R)]q_1 + R[B+A(1+R)]q_2 + (\tau_1+\tau_2)\dot{q}_1 + R\tau_1\dot{q}_2 = -Cf_1 \tag{13}$$

and

$$q_2 = q_1 + \tau_2\dot{q}_1 + (Cf_1 - Df_2) \tag{14}$$

where

$$A = \frac{K_{58}}{K_1+\bar{F}_1}, \qquad B = \frac{\beta}{2\bar{Q}_1(K_1+\bar{F}_1)}$$

$$R^2 = \frac{K_1+\bar{F}_1}{K_2+\bar{F}_2}, \qquad (\dot{\ }) = \frac{\mathrm{d}(\ )}{\mathrm{d}t} \tag{15}$$

$$\tau_1 = \frac{\alpha_{58}}{2\bar{Q}_1(K_1+\bar{F}_1)}, \qquad \tau_2 = \frac{\alpha_{15}}{2\bar{Q}_1(K_1+\bar{F}_1)} \tag{16}$$

and

$$C = \frac{\bar{F}_1}{2(K_1+\bar{F}_1)}, \qquad D = \frac{\bar{F}_2}{2(K_2+\bar{F}_2)} \tag{17}$$

Substituting Eq. (14) into Eq. (13) to eliminate q_2, the dynamic equation for q_1 may be written

$$R\tau_1\tau_2\ddot{q}_1 + G\dot{q}_1 + Hq_1 = -Cf_1 - RS(Cf_1 - Df_2) - R\tau_1(C\dot{f}_1 - D\dot{f}_2) \tag{18}$$

where

$$S = B + A(1+R) \tag{19}$$

and

$$G = \tau_1(1+R) + \tau_2(1+RS), \qquad H = 1+S(1+R) \tag{20}$$

Noting that q_1 is identical to the ratio of fluctuating velocity to mean velocity, Eq. (18) shows that velocity fluctuations in the test section satisfy a second-order equation with complicated forcing due to the coupled action of the two sets of vanes, as represented by the terms on the right side. For given functions f_1 and f_2, q_1 can be found and represented by a Fourier series with coefficients dependent upon both frequency and the various parameters defined in Eqs. (15-17). The main purpose here, however, is to show that the second harmonic amplitude relative to the fundamental can be minimized by proper adjustment of the bypass mean resistance represented by K_2.

While, in principle, the minimum condition can be found for any frequency, only the low-frequency limit will be examined here. Because the response is relatively flat for frequencies sufficiently small compared to the natural frequency given by

$$\omega_0 = \sqrt{H/R\tau_1\tau_2}$$

the limiting case examined subsequently should be applicable for $\omega \ll \omega_0$. Attention is also restricted to the case of identical primary and secondary rotating vanes, i.e., $\bar{F}_2 = \bar{F}_1$. Furthermore, the vanes are operated out of phase so that

$$f_2(\omega t) = f_1(\omega t + \pi)$$

Hence, if the Fourier expansion for $f_1(t)$ is

$$f_1(t) = \sum_{-\infty}^{\infty} a_n e^{in\omega t} \tag{21}$$

where $a_0 = 0$ by definition, i.e., $\bar{f}_1(t) = 0$, then

$$f_2(t) = \sum_{-\infty}^{\infty} a_n e^{in\pi} e^{in\omega t}$$

Noting that $D = R^2 C$, it follows that

$$Cf_1 - Df_2 = C\sum_{-\infty}^{\infty}{}_{n\ \text{odd}} a_n(1+R^2)e^{in\omega t} + C\sum_{-\infty}^{\infty}{}_{n\ \text{even}} a_n(1-R^2)e^{in\omega t} \tag{22}$$

In the low-frequency limit the time derivatives in Eq. (18) may be neglected, and representing q_1 as

$$q_1(t) = \sum_{-\infty}^{\infty} b_n e^{in\omega t} \tag{23}$$

it follows from Eqs. (18) and (21-23), that

$$|b_1| \cong |a_1|\frac{C}{H}|1+RS(1+R^2)|$$

and

$$|b_2| \cong |a_2|\frac{C}{H}|1+RS(1-R^2)|$$

Hence, the ratio of second harmonic to fundamental amplitudes is given by

$$\frac{|b_2|}{|b_1|} = \frac{|a_2|}{|a_1|}\frac{|1+RS(1-R^2)|}{|1+RS(1+R^2)|} \tag{24}$$

For any finite value of R this ratio is such that

$$\frac{|b_2|}{|b_1|} < \frac{|a_2|}{|a_1|}$$

This implies that whenever such a bypass system is used, the harmonic ratio is smaller than that for a conventional design without bypass. To see this, observe that the conventional case is retrieved from the preceding equations by setting $K_2 = \infty$. Then $R = 0$, and

$$\frac{|b_2|}{|b_1|} = \frac{|a_2|}{|a_1|}$$

Equation (24) shows zero second harmonic can be achieved by adjusting R (i.e., K_2) such that

$$1+RS(1-R^2) = 0 \tag{25}$$

In view of Eq. (19), this condition represents a fourth-order equation for R, namely,

$$R^2(R^2-1)A + R(R^2-1)(A+B) - 1 = 0 \tag{26}$$

The root required must be a positive real number. Equation (26) implies that $R > 1$, from which it follows that proper

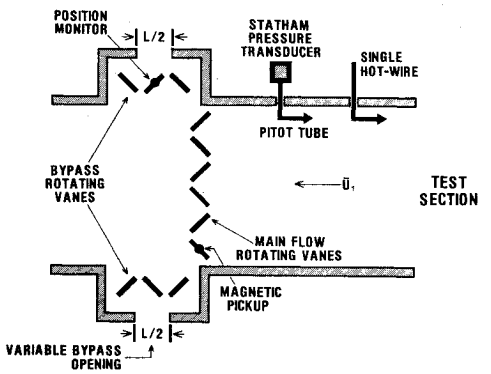

Fig. 2 Test section schematic.

adjustment of K_2 must be such that

$$K_2 < K_1 \tag{27}$$

It should also be noted that the value of K_2 will depend upon A and B, and, hence, upon both the set of vanes chosen and the mean flowrate $\bar{Q}_1$.

III. Experimental Apparatus

The unsteady flow device was installed in the 2×2-ft (0.61×0.61-m) cross section, low-speed wind tunnel at the University of Colorado, Boulder. It is an open-return, suction-type wind tunnel. Figure 1 shows a schematic of the wind tunnel. The test section is 14 ft (4.27 m) in length with a 10-ft long (3.05 m) plexiglass wall, 0.5-in. thick. Downstream of the test section are the unsteady flow device, a transition section to the fan, the fan, and the conical diffuser.

The device consisted of a set of six rotating vanes located just downstream of the test section. Figure 2 shows a schematic of the vane drive apparatus. Three sets of vanes of different widths were used during this experiment to change the amount of maximum tunnel blockage, thus controlling the velocity amplitude. The vanes were made in a modified diamond shape, both for ease of construction and for minimal pressure and friction losses. Of the three sets of vanes, set A had a 2.000-in. chord, set B had a 3.495-in. chord, and set C had a 3.980-in. chord. The three vane sets produced tunnel area blockages of 50, 87.5, and 99.5%, respectively. The rotating vanes were driven by a gear train, which was in turn powered by a General Electric Stratitrol II,§ 0.75 hp, full-wave, dc motor controlled by a Variac-equipped, dc power supply. An 8-to-1 gear reduction allowed the motor to run smoothly near the middle of its 0-1759 rpm speed range preventing surging at low speeds. The gear drive was designed to counter-rotate the vanes, providing zero net local lift perturbation to the flow.

The bypass rotating vane mechanism allowed air to enter the fan section when the test section was blocked by the primary vanes. Three rotating vanes on the top of the device and three on the bottom were driven by the same gear train that drove the primary vanes. The vanes on the top and bottom allowed air from the laboratory to enter the fan section at a varying rate which tended to offset the decreased flow in the test section, providing nearly constant flow through the fan. The adjustment of the bypass mean air flow into the fan section (i.e., K_2) was controlled by movable slides

§Certain commercial equipment, instruments, or materials are identified in this paper in order to adequately specify the experimental procedure. In no case does such identification imply recommendation or endorsement by the U. S. Air Force or National Bureau of Standards, nor does it imply that the material or equipment identified is necessarily the best available for the purpose.

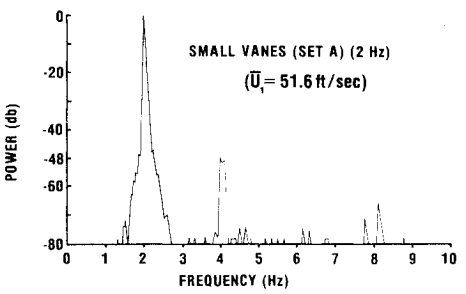

Fig. 3 Power spectrum (ac).

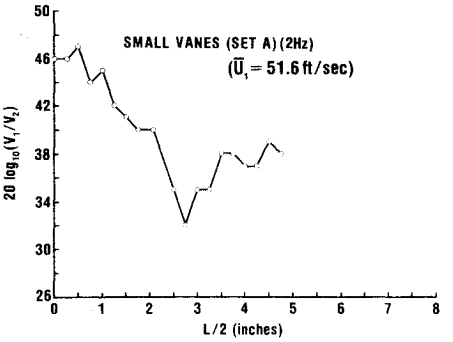

Fig. 4 Difference in first and second harmonic power levels.

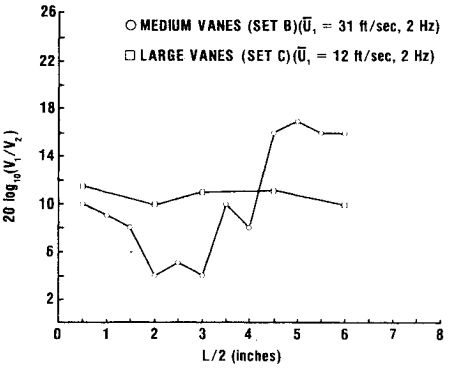

Fig. 5 Difference in first and second harmonic levels.

that are shown in the test section schematic of Fig. 2. These slides were set to predetermined bypass openings (each of length $L/2$) based on the flow conditions desired in the test section. Unlike the primary vanes, the bypass vanes had a fixed 2-in. (5.08 cm) chord, identical to vane set A. Installation of the oscillatory flow device increased the freestream intensity of the longitudinal component of the background turbulence from 0.04 to 0.05% at a freestream speed of 18 m/s.

IV. Experimental Verification of Optimization

Mean and oscillating velocities were measured in the test section using a single-wire constant temperature hot-wire anemometer. The linearized output voltage was ensemble averaged over 50 data entries, with the start of each data-collection cycle being triggered by a magnetic pickup mounted on the vane gear drive. A power spectrum of the resulting signal was produced using a Hewlett-Packard model 5452B Fourier analyzer.

A typical power spectrum of the linearized velocity signal for the small vanes (set A) is shown in Fig. 3 for a rotation rate of 2 Hz, a bypass opening of $L/2 = 1$ in. (2.54 cm), and a mean velocity of 51.6 ft/s (15.6 m/s). The second harmonic power was observed to be approximately 48 dB lower than the

Table 1 Flow parameters - flow reversal measurements

Vane set	$L/2$, in.	T, s	$\bar{U}_1$, ft/s	N, %	k	$Re \times 10^5$	$20 \log_{10}(V_1/V_2)$
A	0.5	0.5	51.6	5.65	0.101	2.241	47
		0.5	36.6	5.15	0.143	1.717	49
B	7.0	0.3	29.5	37.5	0.296	1.383	18
		0.5	31.1	40.0	0.168	1.459	16
		0.7	31.3	47.0	0.119	1.470	10
	3.0	0.5	12.2	59.0	0.429	0.570	13
C	4.5	0.5	11.6	98.0	0.453	0.542	11

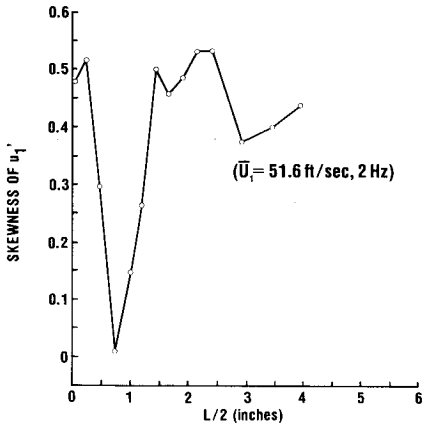

Fig. 6 Skewness of u_1'.

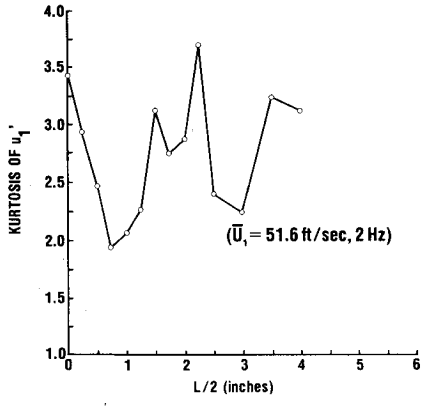

Fig. 7 Kurtosis of u_1'.

power of the fundamental. For the small vanes, usually only the second harmonic was large enough to be detected by the Fourier analyzer on a logarithmic-magnitude power spectrum (maximum scale of 80 dB). The power differences between the fundamental and third harmonic and between the fundamental and fourth harmonic were also noted, if measurable. In no case were they measured to be less than 60 dB and 70 dB, respectively, for the small vanes.

The decibel differences between linearizer output voltages directly related to the first and second harmonics, $20 \log_{10}(V_1/V_2)$, are plotted in Fig. 4 for various values of $L/2$ at this flow condition. For vane set A, at a mean velocity of 51.6 ft/s (15.72 m/s), the optimum or maximum power difference is observed to be approximately 48 dB and the smallest difference is 32 dB. The optimum setting corresponds to $L/2$ slightly less than 1 in.

The power spectrum results for the larger vane sets were not as free from harmonics as those for the smallest vanes. The power differences between the fundamental and second harmonic as functions of $L/2$ are presented in Fig. 5 for both the medium vanes (set B) at a mean velocity of 31 ft/s (9.45 m/s) and for the large vanes (set C) at a mean velocity of 12 ft/s (3.65 m/s). The rotation rate remained at 2 Hz. At these flow conditions, the medium and large vane sets were observed to produce maximum harmonic differences of 15 dB and 11 dB, respectively. The maxima can be clearly distinguished, but they are not as large in magnitude as those measured with the small vane set (set A) installed. It must be remembered that, for mechanical simplicity, only the main-flow vanes were replaced when changing the vane sets; the bypass vanes were not replaced.

The experimental results show that, even with different sizes of main and bypass vanes, a maximum harmonic suppression can be achieved with the proper setting of $L/2$. The required combination of oscillation frequency and amplitude are usually dictated by experimental needs and not by harmonic optimization of the flowfield. The parameters of the unsteady flows produced by each vane set are shown in Table 1. The nondimensional rotation frequency k and the Reynolds number Re are based on an airfoil chord length of 10 in. These data are included to provide comparison with unsteady flow experiments in other wind tunnels.

Harmonic optimization could also be confirmed using the method of Charnay and Mathieu[10] who measured the skewness $\hat{S}$ and kurtosis $\hat{K}$ of the longitudinal turbulent velocity component u_1' in an oscillatory flow tunnel. They found the conditions where $\hat{S}$ approached zero and $\hat{K}$ approached 1.5 represented an optimum. Figures 6 and 7 show the values of kurtosis and skewness vs $L/2$ with the small vanes (set A) for the same flow conditions as considered earlier. It can be seen that the optimum values of $L/2$ are the same as predicted by spectral analysis. Also, the points of maximum $\hat{S}$ and $\hat{K}$ correspond to the points of minimum harmonic suppression.

V. Conclusions

The low-frequency, one-dimensional analysis of the oscillatory wind-tunnel performance demonstrates that an adjustable bypass system with secondary rotating vanes can be used to improve the quality of the waveform of the velocity fluctuations in the test section with respect to that produced by conventional designs, in so far as suppression of second harmonics can be achieved. It also shows that the frequency response improves with increased freestream speed since the time constants vary inversely with speed. By reducing fluctuations in that portion of the tunnel downstream of the primary vanes, the bypass reduces inertial effects (i.e., attenuation) by reducing the effective mass of air that must be accelerated to produce fluctuations. Surging by the fan is also reduced.

The experimental results confirm the feasibility of trimming out second harmonics by proper adjustment of the bypass system. It is felt that the method of analysis should prove beneficial to designers of unsteady wind tunnels, serving as a useful tool for performance prediction and for assessing the effect of various parameters. As an example of the latter, the analysis demonstrates that tunnels with high contraction ratios should have better frequency response because the inertial terms (i.e., the α coefficients) are smaller

than for tunnels with lower contraction ratios (for a given test-section size).

References

[1] McCroskey, W. J. and Philippe, J. J., "Unsteady Viscous Flow on Oscillating Airfoils," *AIAA Journal*, Vol. 13, Jan. 1975, pp. 71-79.

[2] McCroskey, W. J., Carr, L. W., and McAlister, K. W., "Dynamic Stall Experiments on Oscillating Airfoils," *AIAA Journal*, Vol. 14, Jan. 1976, pp. 57-63.

[3] Despard, R. A. and Miller, J. A., "Separation in Oscillating Laminar Boundary Layer Flows," *Journal of Fluid Mechanics*, Vol. 47, Pt. 1, 1971, pp. 21-31.

[4] Saxena, L. S., Fejer, A. A., and Morkovin, M. V., "Effects of Periodic Changes in Free Stream Velocity on Flows Over Airfoils Near Static Stall," *Nonsteady Fluid Dynamics*, proceedings of the Winter Annual Meeting ASME, San Francisco, Calif., Dec. 10-15, 1978, pp. 111-116.

[5] Retelle, J. P., "Unsteady Boundary Layer Flow Reversal in a Longitudinally Oscillating Flow," Frank J. Seiler Research Laboratory, SRL-TR-78-0006, Aug. 1978.

[6] Pierce, G. A., Kunz, D. L., and Malone, J. B., "The Effect of Varying Freestream Velocity on Airfoil Dynamic Stall Characteristics," *Journal of the American Helicopter Society*, Vol. 23, No. 2, April 1978, pp. 27-33.

[7] Despard, R. A., "Laminar Boundary Layer Separation in Oscillating Flow," Ph.D. Thesis, Naval Postgraduate School, Monterey, Calif., June 1969.

[8] Morkovin, M. V., Loehrke, R. I., and Fejer, A. A., "On the Response of Laminar Boundary Layers to Periodic Changes in Freestream Speed," *Proceedings of the Symposium on Recent Research on Unsteady Boundary Layers*, Quebec, 1972.

[9] Karlsson, S. K. F., "An Unsteady Turbulent Boundary Layer," *Journal of Fluid Mechanics*, Vol. 5, May 1959, p. 622.

[10] Charney, G. and Mathieu, J., "Periodic Flow in a Wind Tunnel Produced by Rotating Shutters," *Journal of Fluid Engineering*, Transactions of ASME, Ser. 1, Vol. 98, June 1976, pp. 278-283.